

Assessing risks for integrated water resource management: coping with uncertainty and the human factor

M. J. POLO¹, C. AGUILAR¹, A. MILLARES², J. HERRERO², R. GÓMEZ-BEAS¹,
E. CONTRERAS¹ & M. A. LOSADA²

1 Andalusian Institute of Earth System Research, University of Cordoba. Campus de Rabanales, Edif. Leonardo da Vinci, 14071, Córdoba, Spain
mjpolo@uco.es

2 Andalusian Institute of Earth System Research, University of Granada. Edif. CEAMA, Avda. del Mediterráneo s/n, 18006, Granada, Spain

Abstract Risk assessment for water resource planning must deal with the uncertainty associated with excess/scarcity situations and their costs. The projected actions for increasing water security usually involve an indirect “call-effect”: the territory occupation/water use is increased following the achieved protection. In this work, flood and water demand in a mountainous semi-arid watershed in southern Spain are assessed by means of the stochastic simulation of extremes, when this human factor is/is not considered. The results show how not including this call-effect induced an underestimation of flood risk after protecting the floodplain of between 35 and 78% in a 35-year planning horizon. Similarly, the pursued water availability of a new reservoir resulted in a 10-year scarcity risk increase up to 38% when the trend of expanding the irrigated area was included in the simulations. These results highlight the need for including this interaction in the decision-making assessment.

Key words risk; uncertainty; call-effect; water resource planning

INTRODUCTION

Integrated water resource management requires an accurate assessment of the risks associated with the different soil-use and water-allocation alternatives when planning of resources is being performed. Risk assessment in arid and semi-arid areas must deal with the uncertainty associated with excess/scarcity extreme events occurrence and magnitude, together with the costs associated with their consequences. But the latter is very much dependent on the intervention of man on the territory (Sivapalan *et al.* 2012); the previous actions already performed, devoted to increase water security (e.g. flood mitigation, reservoir storage increase, or even modernization of conduits and irrigation techniques), usually involve an indirect “call-effect”, due to which the territory occupation in the case of flood protection (Di Baldassarre *et al.* 2013), and the associated water use demands when water efficiency is promoted, are increased following the enhanced protection achieved by such actions.

Different sources of uncertainty can be identified when forecasting any objective environmental variable from historical data: measurement and data quality, mathematical structure of models when derived variables are the forecast (Di Baldassarre and Montanari 2012), and the stochastic nature of the input variables to the model. In Mediterranean regions, the high variability of the climate regime makes it necessary to include this source of uncertainty in the forecasting of water-related variables at different spatial and time scales. Provided that the historical datasets quality cannot be changed, once a given model is selected for the forecasting of fluvial water flow, snowmelt, or drought duration, the occurrence and magnitude of the weather/hydrological variables remain as the main source of uncertainty in hydrological and water resource simulations.

Uncertainty assessment of hydrological variables can be performed from different approaches (Aven 2008), Monte Carlo techniques being widely used, among others, for resampling input variables and/or parameters in physical/empirical and distributed/lumped models, from simple to more sophisticated algorithms (e.g. Khu and Werner 2003, Baquerizo and Losada 2008, No *et al.* 2011, Gómez-Beas *et al.* 2012). This work shows representative examples of situations in Mediterranean watersheds in which the human factor must be considered when analysing the benefit associated with water security actions: flooding and water demand in a selected site in southern Spain are assessed by means of the stochastic simulation of extremes in the medium and short term; the comparison of the different results derived when the human factor is/is not considered is completed with risk quantification for selected situations.

STUDY SITE DESCRIPTION AND AVAILABLE DATA

The Guadalfeo River watershed is a 1350-km² coastal watershed in Granada, Spain (Fig. 1) where both alpine and subtropical climates can be found in the 60-km distance from the Sierra Nevada mountains (higher than 3000 m) to the Mediterranean coastline, which has resulted in a high heterogeneity of soil uses and water-demanding activities. Table 1 includes some climate and soil use descriptors of the area. The cyclic sequences of drought and wet periods usually mean water demands are not satisfied, and associated economic losses of crop production or flood damage. In 2002, a big dam (Rules Reservoir) was built to guarantee irrigation water for the tropical crops distributed throughout the southern area of the watershed, and to provide the coastal towns with water resource for tourism development. Upstream of the dam, at Órgiva, local floods occur when direct runoff from torrential rainfall is increased by significant snowmelt flows, and bank protection actions have been projected to decrease flood damage in the area.

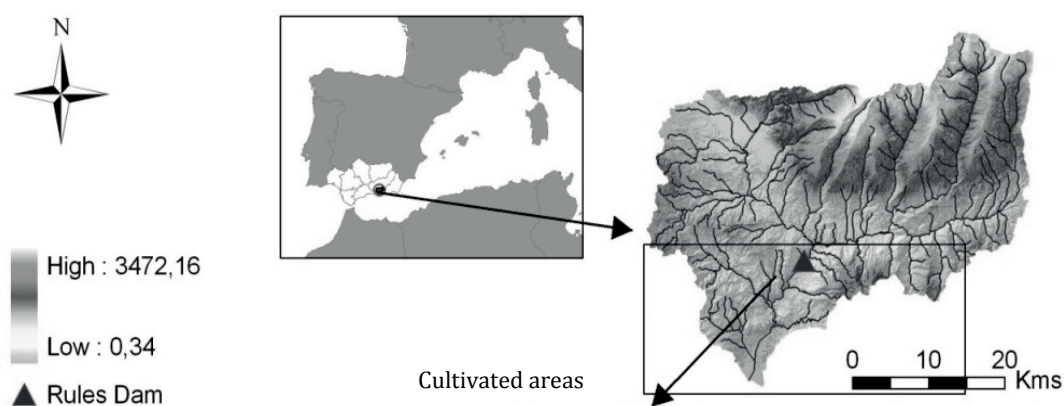


Fig. 1 Study site location and Digital Elevation Model (m).

Table 1 Climatic and water demand descriptors at the Guadalfeo River Basin, related to water supply from the Rules Reservoir.

Climatic descriptors ¹		Soil-use/water demands	
Precipitation (mountain areas)	630 mm year ⁻¹	Urban supply	13 hm ³ year ⁻¹
Precipitation (valley areas)	460 mm year ⁻¹	Irrigation demand	113.62 hm ³ year ⁻¹
Temperature (mountain areas)	6.5°C (2.5–19°C)	Ecological flow	1 m ³ s ⁻¹
Temperature (valley areas)	15.1°C (15–40°C)	Hydropower	2.5 m ³ s ⁻¹
River flow to Rules dam	4 m ³ s ⁻¹ (0.13–112.4 m ³ s ⁻¹)		

¹ Average values for 2000–2012 period; values in brackets stand for the range interval.

The reservoir operation provides users with the following decreasing priority: urban demand (domestic uses), ecological regime, irrigation, and hydropower. Different previous works had studied the impact of the reservoir on this area, which included the hydrological modelling of the contributing watershed (Herrero *et al.* 2009; Millares *et al.* 2009; Aguilar *et al.* 2010; Polo *et al.* 2010) and the operability of the reservoir management in terms of water supply (Gómez-Beas *et al.* 2012).

INCLUDING THE HUMAN FACTOR IN FLOOD RISK ASSESSMENT: A SIMPLE EXAMPLE

In previous work, Polo and Losada (2010) derived the flooding probability maps at Órgiva, upstream of the reservoir, in a 35-year period. *F* was defined as the probability of a point being flooded at least once in a 35-year horizon. *F* mapping was estimated from the flooded area associated with the 35-year peakflow, *Q*, regime, defined by its cumulative distribution function, *p* ($F = 1 - p$ along the limits of the associated flood area). Figure 2(a) shows the empirical

cumulative distribution function of $Q(p)$ at the study site, obtained from the available 35-year daily precipitation data in the watershed and the 20-year daily flow data and annual maximum instantaneous flow at the study site (Polo and Losada 2010). For instance, the maximum Q value in 35-year was estimated by adopting $p = 0.99$ as $190 \text{ m}^3\text{s}^{-1}$ (Q_{maximum}). The flooding area for a given Q value (i.e. p or F value) was then calculated by means of hydrodynamic modelling. Bank protection actions have been projected to decrease flood damage in this area, after which Q values lower than $65 \text{ m}^3\text{s}^{-1}$ ($Q_{\text{threshold}}$) will cause no flooding. Figure 2(b),(c) also show the flood area maps for Q_{maximum} and $Q_{\text{threshold}}$. Without the actions, F is a continuous variable decreasing from 1 in the longitudinal axis of the river (dark line) to 0.01 in the both-sided limits of the $190 \text{ m}^3 \text{ s}^{-1}$ flooding area, even lower for higher Q values (wider limits).

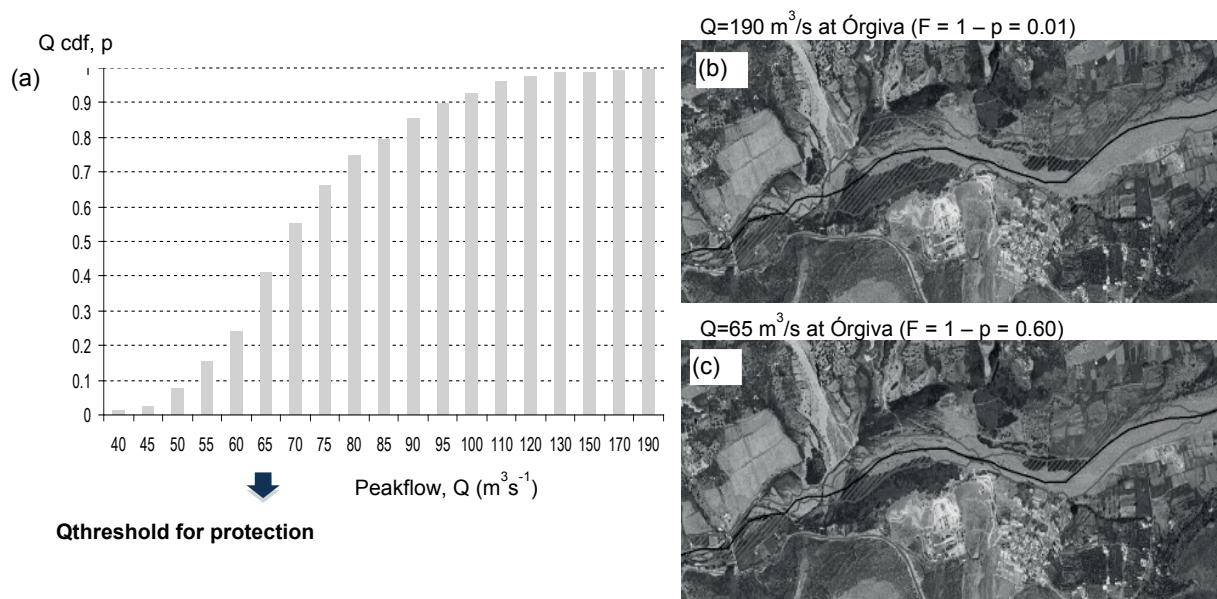


Fig. 2 Empirical cumulative distribution function of Q , and two examples of flood area maps (Polo and Losada 2010).

To assess the impact of these actions on the final F map, an F value of 0.6 was obtained from Fig. 2, associated to this water flow threshold ($Q_{\text{threshold}} = 65 \text{ m}^3 \text{ s}^{-1}$, $p = 0.4$) over which the protection is useless. For the area beyond $F = 0.6$ lines (Figure 2(c)), the value of F after the protection actions (F_{after}) does not change ($F_{\text{after}} = F$), but the enclosed area will not be flooded unless water flow is higher than $Q_{\text{threshold}}$, that is, $F_{\text{after}} = 0.6$ throughout this area. F is then directly affected by the extent of the actions. Risk (R) evaluation at a given point requires a quantification of the local damage (D) caused by floods ($R = F \cdot D$). R after the protection action does not change out of the protected area with respect to its former value, but it drops to a constant expression ($R = 0.6D$) within the protected area. To assess the human factor influence on risk evaluation at a given point, a simple estimation of damage can be done in terms of the degree of occupation of the territory at that point, C . The call-effect induced by the protection action is quantified by comparing C values before and after the action. In this work, a simple hypothesis has been adopted: C_{after} is higher than C_{before} ($C_{\text{after}} = f \cdot C_{\text{before}}$; $f > 1$) within the protected area, and it remains unchanged out of these limits.

Risk assessment: results

The expected flood risk at the study site after the protection actions, R , was assessed taking the Q_{maximum} flood area ($Q = 190 \text{ m}^3\text{s}^{-1}$) as reference area, and estimating R variation when the human factor described above was/was not included (R_{with} , R_{without}). The R_{without} and R_{with} maps can be estimated by multiplying the F map after the action by the estimated C_{without} and C_{with} maps, respectively. The resulting R_{with} and R_{without} maps will just differ within the limits of the protected

area, where $R_{\text{with}} = f \cdot R_{\text{without}}$. To estimate the global impact of the human factor in risk estimation at the study site, the averaged values of R_{with} and R_{without} were compared. If a is the fraction of protected area at the study site ($1 - a$, the non-protected area fraction), $R_{\text{with},a}$ and $R_{\text{with},1-a}$ the averaged R_{with} in the protected and non-protected area, and $R_{\text{without},a}$ and $R_{\text{without},1-a}$ the averaged R_{without} in the protected and non-protected area, respectively, the averaged R_{with} , and R_{without} over the reference area can be written as $R_{\text{without,avg}} = aR_{\text{without},a} + (1-a)R_{\text{without},1-a}$, and $R_{\text{with,avg}} = aR_{\text{with},a} + (1-a)R_{\text{with},1-a} = a f R_{\text{without},a} + (1-a)R_{\text{without},1-a}$. The final $R_{\text{with,avg}}/R_{\text{without,avg}} = (1 + f A B)/(1 + A B)$, with $A = a/(1-a)$ and $B = R_{\text{without},a}/R_{\text{without},1-a}$, is always higher than unity, whatever a and f are. The underestimation of risk when the human factor is not considered is therefore dependent on the initial gradient of the final risk (after the protection action) throughout the study area, as $B = R_{\text{without},a}/R_{\text{without},1-a}$ can significantly vary depending on the initial distribution of C in the territory and F decreases with the distance to the river. For the simple modelling of the human factor adopted in this work, it can be observed that $R_{\text{with,avg}}/R_{\text{without,avg}}$ tends to reach f as B increases. To illustrate this, an effective value of $f = 5$ was assumed in the study area, taking into account the current occupation of the territory and the observed trends in similar areas after protection actions in river banks. Since the flood area for $Q = 65 \text{ m}^3\text{s}^{-1}$ is 55% of the flood area for $Q = 190 \text{ m}^3\text{s}^{-1}$ (reference area), it is easy to obtain $A = 0.55/0.45 = 1.222$. Figure 3(a) shows the variation of the resulting $R_{\text{with,avg}}/R_{\text{without,avg}}$ with increasing B values for $f = 5$, with a maximum underestimation of a 80% when the human factor is not included. For a given B value, $R_{\text{with,avg}}/R_{\text{without,avg}}$ increases with f , as expected (Figure 3(b)); for $f = 1.5$, a maximum underestimation of a 33% is found.

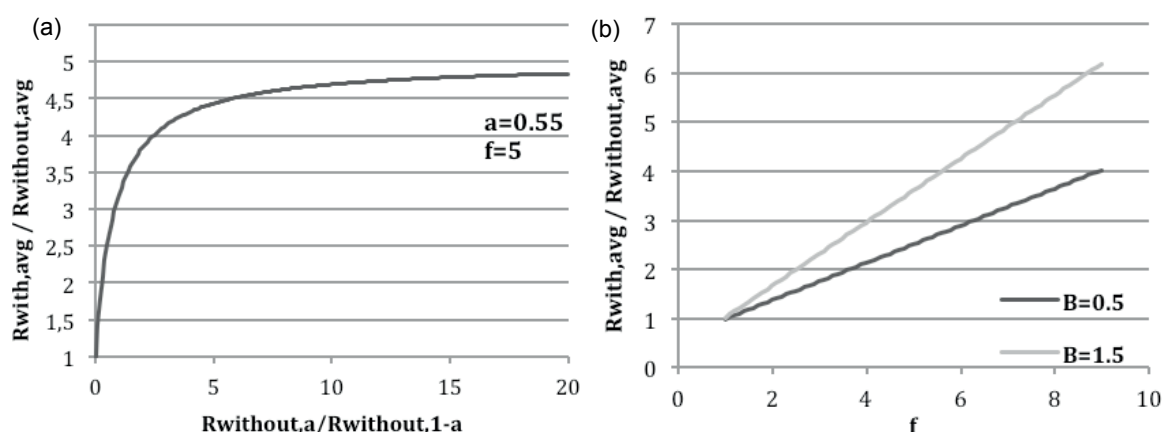


Fig. 3 Variation of $R_{\text{with,avg}}/R_{\text{without,avg}}$ with B (a) and f (b) for the study area ($a = 0.55$; $A = 1.22$).

The final values of risk, both locally or globally calculated at a given study area, should of course consider more complex models of damage-cost quantification. Not only occupation of the territory, but also different kinds of soil use are usually changed when protection is increased, and f and D values can be highly variable throughout a given area. Moreover, the enhanced value of the now protected area will likely change over time, not at once. However, the simple hypothesis adopted in this work shows the significance of the human factor in risk evaluation after protection actions and how this must be considered for the evaluation of adaptation-mitigation strategies.

INCLUDING THE HUMAN FACTOR IN IRRIGATION GUARANTEE RISK ASSESSMENT

Gómez-Beas *et al.* (2012) tested the operability of the different operation criteria used by the reservoir management system, which are currently expressed in terms of the minimum storage to be maintained (equivalent to a minimum number of days with water supply), by means of estimating the frequency of failure to maintain this guarantee in a 10-year planning horizon. Synthetic series of daily water inflow to the reservoir were simulated in their work by resampling the available dataset with the Monte Carlo technique, and they were used as input to a lumped reservoir model for the

water balance that included operation criteria. Irrigation supply efficiency was tested by using some local criteria included in the Hydrological Plan of the South Basin in Spain.

The probability of failure in water supply from the Rules Reservoir was assessed under different operational criteria for both the current irrigation demand and the inclusion of the human factor. The call-effect was now considered by means of an increasing trend over the 10-year study period, due to an increase of irrigated crop surface induced by the availability of water storage. A linear increase up to twice the current demand was considered over the first five years, which was maintained as constant during the rest of the period. This trend was estimated from the irrigation increase observed in the Guadalquivir River Basin following the increase in water storage during the past 50 years (Contreras and Polo 2011). The other demands were not changed for this study. Daily water inflow to the reservoir and the evolution of water storage under both situations, current irrigation demand and increased demand, were simulated following the methodology developed in Gómez-Beas *et al.* (2012), and probability functions for different irrigation supply efficiency parameters were derived. These parameters are used as irrigation supply warranty criteria: (1) irrigation volume supply in 1 year being higher than 40% of demand, (2) irrigation volume supply in 2 years being higher than 60% of demand, and (3) irrigation volume supply in 10 years being higher than 80% of demand. Figure 4 shows the cumulative distribution functions obtained for the failure in Warranty-1 and 2 criteria under irrigation area increase (scenario 1) and under no increase (scenario 2), for different operational criteria expressed as minimum storage in the reservoir (number of days with guaranteed supply for urban demand). As can be observed, the operational criteria themselves do not generate significant differences in the estimated probability of failure in irrigation warranty, but the increase of irrigation demand involves a non-negligible increase of probability of failure.

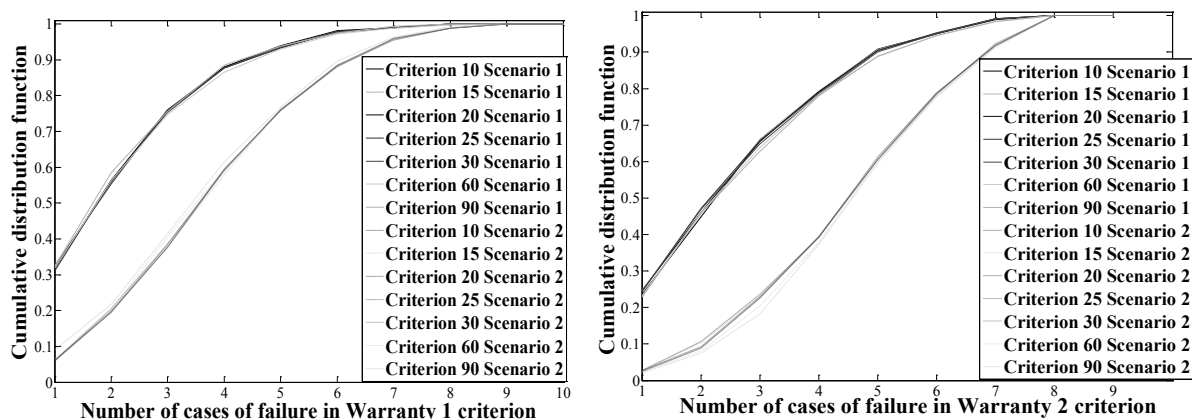


Fig. 4 Empirical cumulative distribution functions for the number of years in a 10-year period with no compliance of the defined irrigation warranty criterion 1 and 2, with and without an increase of irrigation demand (scenario 1 and 2, respectively).

The warranty criterion 3 is never accomplished with the estimated increase trend over the 10 years (scenario 1), and very rarely accomplished without such an increase in the irrigation demand (scenario 2) with failure probability values ranging from 0.08 for the operational 10-days criterion to 0.20 for the operational 90-days criterion. Risk increase under scenario 1 (irrigation area increase) was assessed for a medium operational 60-days criterion. From the simulation results, the empirical cumulative distribution functions for the increase of failure in irrigation water supply in two time horizons, 2 and 10 years, are shown in Fig. 5. From the results, the probability of no increase of risk considering the increase of irrigated area in 2 years is 0.264, but 0 over the whole 10-year study period. A mean value of 11 and 590 hm^3 of additional deficit in irrigation supply under this scenario were obtained for 2 and 10 years, respectively, against mean deficits of 26 and 261 hm^3 for the same periods when no increase in irrigation area (scenario 2) is included in the analysis. Assuming an uniform unitary cost per unit of irrigation area not being supplied, also

constant over the 10 years, the risk associated to an additional failure of 11 hm³ in 2 years due to the increase trend in irrigated area is a 38% of the average risk in 2 years, but it may increase up to a 226% over 10 years.

If a variable cost was considered in the analysis, the final numbers would be different. However, the main purpose of this work was to quantify the influence of the call-effect in the risk estimations, and additional sources of variation were not included. Finer approximations can be performed for both the uncertainty analysis and costs estimations, which must be locally dependent.

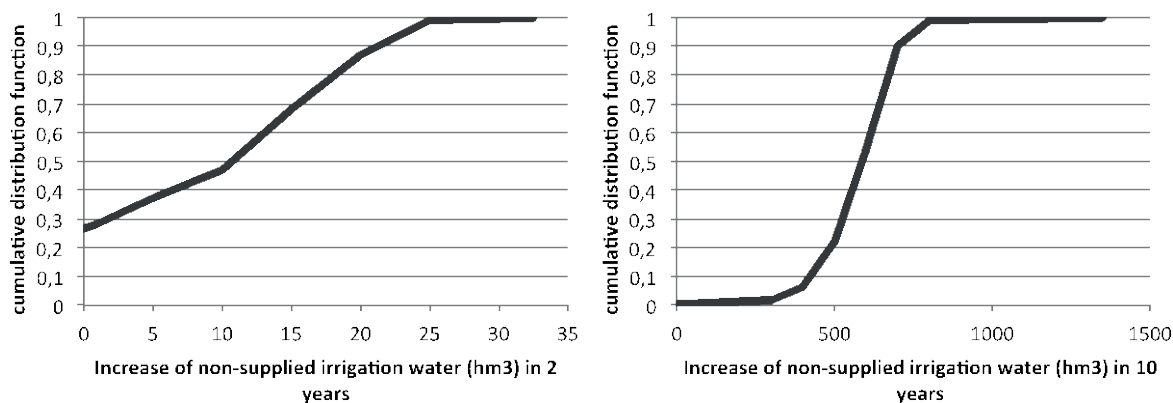


Fig. 5 Empirical cumulative distribution functions for the increase of failure in water supply for 60-days operational criterion and scenario 1.

CONCLUSIONS

Uncertainty assessment and risk analysis can be powerful tools to support the decision making process in water resource planning and management. However, when assessing the potential benefits of actions devoted to increase water security, the human factor must be included in the *a priori* analysis, since the observed call-effect associated with the development of protection actions against floods or water scarcity involves a significant increase in the probability and damage estimations for different extreme events, and a final increase of risk.

From the results, it is possible to fix the thresholds for the variables quantifying the call-effect (e.g. occupation of the territory, irrigated area) that can be assumed by the system, if any, by adopting a maximum risk level to be assumed, and to promote legal or administrative regulations to prevent an excess increase of the soil and water demands that imbalance the expected benefits from adaptation/mitigation actions.

REFERENCES

- Aguilar, C., Herrero, J. and Polo, M. J. (2010) Topographic effects of solar radiation distribution in mountainous watershed and their influence on reference evapotranspiration estimates at watershed scale. *Hydrol. Earth Syst. Sci.* 14, 2479–2494.
- Aven, T. (2008) *Risk Analysis: Assessing Uncertainties Beyond Expected Values and Probabilities*. Wiley, Chichester.
- Baquerizo, A. and Losada, M. A. (2008) Human interaction with large scale coastal morphological evolution. *Coastal Engineering* 55, 569–580.
- Di Baldassarre, G. and Montanari, A. (2012) Data errors and hydrological modelling: the role of model structure to propagate observation uncertainty. *Advances Water Resources*, doi: 10.1016/j.advwatres.2012.09.007.
- Di Baldassarre, G., et al. (2013) Socio-hydrology: conceptualising human-flood interactions. *Hydrol. Earth Syst. Sci.* 17, 3295–3303.
- Contreras, E. and Polo, M. J. (2011) Propuesta metodológica para diagnosticar y pronosticar las consecuencias de las actividades humanas al estuario del Guadalquivir. Capítulo 2: Aportes desde la cuenca vertiente. Technical Report (in Spanish), pp 123.
- Gómez-Beas, R., Moñino, A. and Polo, M. J. (2012) Development of a management tool for reservoirs in Mediterranean environments based on uncertainty analysis. *Nat. Hazards Earth Syst. Sci.* 12, 1789–1797.
- Herrero, J., et al. (2009) An energy balance snowmelt model in a Mediterranean site. *J. Hydrol.* 371, 98–107.
- Khu, S. T. and Werner, M. G. F. (2003) Reduction of Monte Carlo simulation runs for uncertainty estimation in hydrological modelling. *Hydrol. Earth Syst. Sci.* 7(5), 680–692.
- Millares, A., Polo, M. J. and Losada, M. A. (2009) The hydrological response of baseflow in fractured mountain areas. *Hydrol. Earth Syst. Sci.* 13, 1261–1271.

- Noh, S. J., *et al.* (2011) Applying sequential Monte Carlo methods into a distributed hydrologic model: lagged particle filtering approach with regularization. *Hydrol. Earth Syst. Sci.* 15, 3237–3251.
- Polo, M. J. and Losada, M. A. (2010) Uncertainty assessment for long-term forecasting of extreme values in streamflow due to catchment changes in a Mediterranean mountainous watershed in Southern Spain. HydroPredict 2010, Prague, September 20–23.
- Polo, M. J., *et al.* (2010). WiMMed, a distributed physically-based watershed model (I): description and validation. In: *Environmental Hydraulics. Theoretical, experimental and computational solutions* (ed. by P. A. López-Jiménez *et al.*), 225–232. CRC Press/Balkema, Chippenham.
- Sivapalan, M., Savenije, H. H. and Blöschl, G. (2012) Socio-hydrology: a new science of people and water. *Hydrol. Processes* 26, 1270–1276.